文章编号:1671-6833(2023)01-0052-06

推进轴系纵向高承载准零刚度隔振器的研究

任志英[1,2], 邱 涛[1,2], 刘扭扭[1,2], 白鸿柏[1,2], 尧杰程[1,2], 梁 翼[1,2]

(1. 福州大学金属橡胶与振动噪声研究所,福建 福州 350116; 2. 福州大学 机械工程及自动化学院, 福州 350116)

摘 要: 针对船舶推进轴系纵向低频隔振难的问题,将具备负刚度特性的碟簧与正刚度螺旋弹簧并联,设计了一种高承载准零刚度隔振器。建立了轴系-准零刚度隔振系统的动力学方程,利用谐波平衡法求解了系统的稳态响应,并用数值方法验证了求解的有效性。对于系统响应稳定性的问题,首先研究了准零刚度隔振器的非线性刚度、外激励力幅值对系统响应稳定性的影响规律,并结合推进轴系的纵向静变形限制,确定了非线性刚度取值;其次基于静力学理论设计了一组碟簧与螺旋弹簧的结构参数;最后分析了准零刚度隔振器的阻尼比、外激励力幅值对系统响应稳定性的影响规律,并确定了合适的阻尼比。结果表明:当非线性刚度、阻尼比分别设计为 1×10^{12} N/m^3、0.05 时,系统主共振不再出现跳跃现象,稳态响应的解在 200 Hz 内都是稳定的;在承受 10 000 N 载荷时,准零刚度隔振器仍然可以有效隔离 10~200 Hz 低频段的振动。

关键词: 推进轴系; 低频隔振; 碟簧; 准零刚度; 稳定性

中图分类号: TH113.1 **文献标志码**: A **doi**:10.13705/j.issn.1671-6833.2022.04.019

船舶运行过程中,推进轴系产生的纵向振动会严重影响船舶可靠性与静谧性[1]。相较于主动隔振,被动隔振方案可靠性更高、结构简单,更适用于推进轴系的纵向隔振。Goodwin[2]在上世纪 60 年代首先利用共振转换器来减小推进轴系的纵向振动,并取得了良好的效果。随后国内外相关学者对共振转换器的轴向隔振性能进行了更深入的研究[3-7],在推进轴系纵向振动的控制中取得了较好的成果,但是难以满足实际中越来越严格的低频隔振要求。

准零刚度隔振器由正负刚度元件并联组成,拥有优秀的低频隔振性能[8]。并联机构的负刚度特性可以通过引入组合的螺旋弹簧[9]、连杆与水平弹簧机构[10]、欧拉屈服梁[11]、剪式连杆机构[12]、凸轮滚子弹簧机构[13]等来实现。由以上负刚度元件构建的准零刚度隔振器虽然能有效隔离低频振动,但是并不适用于要承受大载荷且轴向空间受限的推进轴系。碟形弹簧具有非线性刚度的特点,碟簧的高厚比大于$\sqrt{2}$时具备负刚度特性,此时将碟簧与螺旋弹簧并联构建的准零刚度隔振器不仅低频隔振效果好,并且承载能力强、结构紧凑[14-16],更适于轴向空间小的场合。因此本文将具备负刚度特性的碟簧与螺旋弹簧并联,构建一种高承载准零刚度隔振器。通过对隔振系统稳定性的分析,确定了准零刚度隔振器的非线性刚度与阻尼比,并设计了碟簧与螺旋弹簧的参数,最后验证了其低频隔振性能。

1 准零刚度隔振器布置方案

图 1 为碟簧-螺旋弹簧并联实现的准零刚度隔振器。当碟簧的压缩量达到 Δf 时,碟簧在该平衡点附近产生的负刚度正好抵消螺旋弹簧的正刚度,机构的总刚度为零,此时可以有效隔离低频振动。

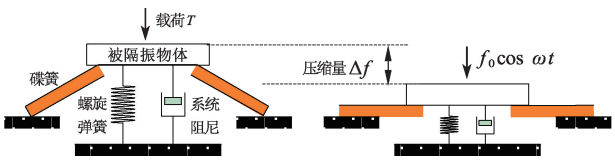

图 1 碟簧-螺旋弹簧并联示意图

Figure 1 Schematic diagram of parallel connection of disc spring and coil spring

引入上述准零刚度隔振器后,推进轴系纵向低频隔振方案的示意图如图 2 所示。轴系被简化为一

收稿日期:2021-11-02;**修订日期**:2022-01-09

基金项目:国家自然科学基金资助项目(52175162);福建省自然科学基金资助项目(2019J01210)

作者简介:任志英(1980—),女,浙江嵊州人,福州大学教授,博士,博士生导师,主要从事金属橡胶材料设计、减振降噪技术等研究,E-mail:renzyrose@126.com。

引用本文:任志英, 邱涛, 刘扭扭,等. 推进轴系纵向高承载准零刚度隔振器的研究[J]. 郑州大学学报(工学版),2023,44(1):52-57. (REN Z Y, QIU T, LIU N N, et al. Research on longitudinal high load-bearing quasi-zero stiffness isolator for propulsion shafting[J]. Journal of Zhengzhou university (engineering science),2023,44(1):52-57.)

等截面轴,轴系结构参数长度、直径、弹性模量、材料密度分别用 L、D_1、E、ρ 表示;推力盘的质量用 m_{th} 表示;准零刚度隔振器的质量与阻尼分别用 m_2、c_2 表示,其在静平衡位置处提供的回复力用 $\tilde{f}$ 表示。

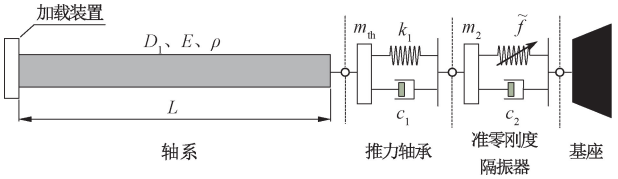

图 2　推进轴系纵向低频隔振示意图

Figure 2　Schematic diagram of longitudinal low frequency vibration isolation of propulsion shafting

2　轴系纵向动力学分析

2.1　动力学方程建立与求解

根据图 2 建立了轴系-准零刚度隔振器的动力学模型,如图 3 所示。在研究低频范围内轴系纵向振动时可以将其简化为单自由度,用质量 m_1 表示;在平衡位置处,准零刚度隔振器的回复力与位移可以近似为三次方关系,并用 k_{qzs} 表示非线性刚度;由于基座刚性大,因此可以将基座视为固定端;其他符号意义与第 1 节相同。

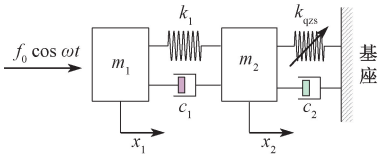

图 3　轴系-准零刚度隔振器动力学模型

Figure 3　Shafting-quasi-zero stiffness isolator dynamic model

图 3 的动力学方程可写成:

$$\begin{cases} m_1\ddot{x}_1 + k_1(x_1 - x_2) + c_1(\dot{x}_1 - \dot{x}_2) = f_0\cos\omega t; \\ m_2\ddot{x}_2 - k_1(x_1 - x_2) - c_1(\dot{x}_1 - \dot{x}_2) + c_2\dot{x}_2 + k_{qzs}x_2^3 = 0。 \end{cases} \tag{1}$$

令 $X_i = \dfrac{x_i}{D_1}$,$\zeta_i = \dfrac{c_i}{2m_1\omega_1}$,$K_{qzs} = \dfrac{k_{qzs}}{k_1}D_1^2$,$T = \omega_1 t$,

$F_0 = \dfrac{f_0}{k_1 D_1}$,$\omega_1 = \sqrt{\dfrac{k_1}{m_1}}$,$\beta = \dfrac{m_2}{m_1}$,$\Omega = \dfrac{\omega}{\omega_1}$,则式(1)可写成如下无量纲方程:

$$\begin{cases} \ddot{X}_1 + X_1 - X_2 + 2\zeta_1(\dot{X}_1 - \dot{X}_2) = F_0\cos\Omega T; \\ \beta\ddot{X}_2 - X_1 + X_2 - 2\zeta_1(\dot{X}_1 - \dot{X}_2) + 2\zeta_2\dot{X}_2 + K_{qzs}X_2^3 = 0。 \end{cases} \tag{2}$$

设该系统的稳态响应解为

$$\begin{cases} X_1 = C_1\cos\Omega T + S_1\sin\Omega T; \\ X_2 = C_2\cos\Omega T + S_2\sin\Omega T。 \end{cases} \tag{3}$$

将式(3)代入式(2)中,采用谐波平衡法进行求解,仅保留一次谐波项,并令各谐波项系数相等可得

$$\begin{cases} C_1 - \Omega^2 C_1 - C_2 + 2\zeta_1\Omega S_1 - 2\zeta_1\Omega S_2 = F_0; \\ S_1 - \Omega^2 S_1 - S_2 + 2\zeta_1\Omega C_2 - 2\zeta_1\Omega C_1 = 0; \\ C_2 - C_1 - \beta\Omega^2 C_2 + 2\zeta_1\Omega(S_2 - S_1) + \\ \quad 2\zeta_2\Omega S_2 + \dfrac{3}{4}K_{qzs}C_2(C_2^2 + S_2^2) = 0; \\ S_2 - S_1 - \beta\Omega^2 S_2 + 2\zeta_1\Omega(C_1 - C_2) - \\ \quad 2\zeta_2\Omega C_2 + \dfrac{3}{4}K_{qzs}S_2(C_2^2 + S_2^2) = 0。 \end{cases} \tag{4}$$

解析解可通过求解式(4)获得。

2.2　求解有效性的验证

本文中轴系结构参数 $L = 3$ m,$D_1 = 0.08$ m,$E = 206\,000$ MPa,$\rho = 7\,800$ kg/m^3,并取 $k_{qzs} = 1 \times 10^{13}$ N/m^3、$f_0 = 75$ N、$\zeta_1 = 0.02$、$\zeta_2 = 0.02$、$\beta = 0.1$ 来验证解析法求解的有效性。用四阶龙格-库塔法求解方程(2),x_2 的幅值用 A_2 表示。解析解与数值解的结果对比如图 4 所示,可以看出数值解与解析解的吻合度高,说明用谐波平衡法进行求解是可行的。

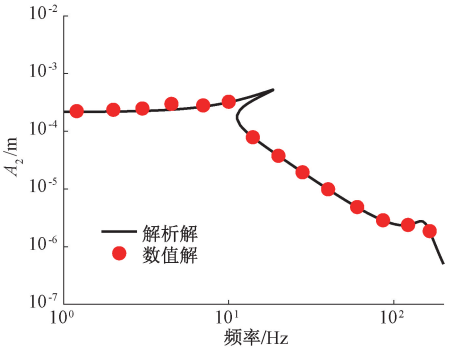

图 4　解析解与数值解对比

Figure 4　Analytical solutions compared with numerical solutions

2.3　系统力传递率曲线

用力传递率来评价准零刚度隔振器的隔振性能。力传递率定义为 $T_f = f_t/f_0$,其中 f_t 为传递到基座上的力,f_0 为激励力幅值,并将传递率转换为分贝的形式,即 $20\lg\ T_f$,无隔振器系统与加入隔振器系统的力传递率曲线如图 5 所示,无隔振器系统的起始隔振频率为 65.7 Hz;加入隔振器的系统的起始隔振频率为 18.5 Hz,且在 18.5~200 Hz 频段内力传递率相较于无隔振器系统大幅降低。

3　准零刚度隔振器参数对系统稳定性的影响

准零刚度隔振器具备优秀的低频隔振性能,但在实际运用中,其非线性特点可能会影响实际的隔

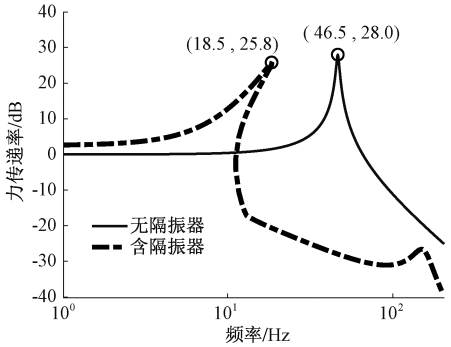

图 5 力传递率曲线

Figure 5 Force transmission rate curve

振效果,因此,分析系统的稳定性是十分有必要的。对式(2)求得的稳态解施加一个小扰动,方程的解可以写成:

$$\tilde{X}_i = X_i + u_i。\tag{5}$$

式中:X_i 表示方程(2)的稳态解,$i=1,2$。

将式(5)代入式(2)中并忽略高阶的非线性项,得到如下关于小扰动 u_i 的线性化方程:

$$\begin{cases}\ddot{u}_1 + u_1 - u_2 + 2\zeta_1(\dot{u}_1 - \dot{u}_2) = 0;\\ \beta\ddot{u}_2 - u_1 + u_2 - 2\zeta_1(\dot{u}_1 - \dot{u}_2) + \\ \qquad 2\zeta_2\dot{u}_2 + 3K_{qzs}X_2^{\ 2}u_2 = 0。\end{cases}\tag{6}$$

设方程(6)的解为如下形式:

$$\begin{cases}u_1 = a_1\cos\Omega T + b_1\sin\Omega T;\\ u_2 = a_2\cos\Omega T + b_2\sin\Omega T。\end{cases}\tag{7}$$

将式(7)代入方程(6)中并保留一次谐波项,令其各谐波项的系数等于 0 可得如下方程:

$$\begin{cases}(1-\Omega^2)a_1 + 2\Omega\zeta_1 b_1 - a_2 - 2\Omega\zeta_1 b_2 = 0;\\ (1-\Omega^2)b_1 - 2\Omega\zeta_1 a_1 - b_2 + 2\Omega\zeta_1 a_2 = 0;\\ \left(1-\beta\Omega^2+\dfrac{9}{4}K_{qzs}X_2^2\right)a_2 - 2\Omega\zeta_1 b_1 + \\ \qquad 2\Omega(\zeta_1+\zeta_2)b_2 - a_1 = 0;\\ \left(1-\beta\Omega^2+\dfrac{3}{4}K_{qzs}X_2^2\right)b_2 + 2\Omega\zeta_1 a_1 - \\ \qquad 2\Omega(\zeta_1+\zeta_2)a_2 - b_1 = 0。\end{cases}\tag{8}$$

将式(8)写成矩阵形式 $\boldsymbol{A}[a_1 \quad b_1 \quad a_2 \quad b_2]^{\mathrm{T}} = 0$,若矩阵 $\boldsymbol{A}$ 的行列式 $\Delta < 0$,则系统的响应是不稳定的。

3.1 非线性刚度对系统稳定性的影响

讨论不同非线性刚度对系统响应稳定性的影响时,取阻尼比 $\zeta_2 = 0.03$ 进行分析。图 6(a)、6(b)、6(c)分别表示不同非线性刚度下,系统的幅频响应与不稳定区间,其中虚线为系统的不稳定边界,边界内部为系统的不稳定区间。图 6(d)表示激励力幅值为 75 N 时,系统的幅频响应随非线性刚度变化的曲线。

由图 6 可知,当非线性刚度一定时,激励力幅值越小,系统幅值的响应越小,且起始隔振频率也越低。此外系统不稳定解的区间也会随着激励力幅值的减小而减小。激励力幅值一定时,系统的非线性

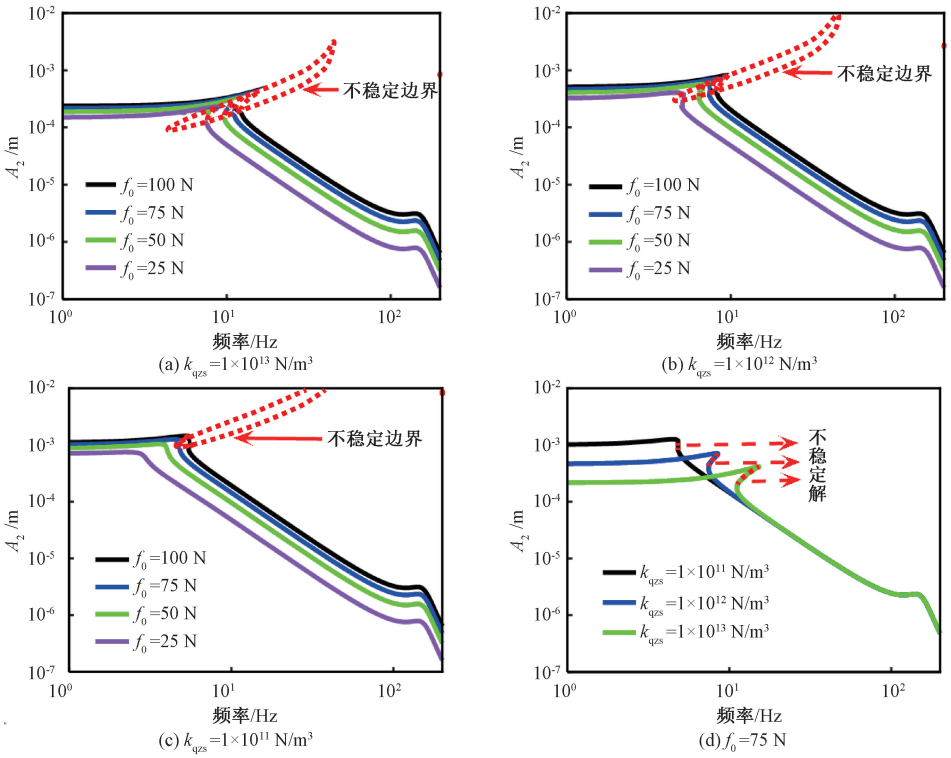

图 6 不同非线性刚度幅频响应与稳定性图

Figure 6 Amplitude-frequency response and stability diagram of different nonlinear stiffness

刚度越大,对应的起始隔振频率也越高,不稳定的跳跃现象越明显,较小的非线性刚度能避免系统的响应出现过大的不稳定区间。但在实际中考虑到艉轴承密封的要求,推进轴系的轴向静变形有一定限制[17],这表明非线性刚度不宜选取过小。综上所述,选取非线性刚度为 1×10^{12} N/m^3。

3.2　碟簧与螺旋弹簧的设计

确定非线性刚度后,可根据相关静力学理论设计碟簧与螺旋弹簧结构参数。碟形弹簧示意图如图 7 所示。

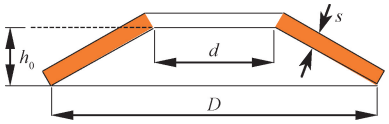

图 7　碟形弹簧示意图

Figure 7　Schematic diagram of disc spring

常用碟簧的载荷-位移曲线可以根据 A-L 解[18]近似求出:

$$F=\frac{4Es^3f}{(1-\mu^2)MD^2}\left[\left(\frac{h_0}{s}-\frac{f}{s}\right)\left(\frac{h_0}{s}-\frac{f}{2s}\right)+1\right]。\tag{9}$$

式中:E 为弹性模量,MPa;μ 为泊松比;f 为碟簧的压缩量,mm;D、d 分别为碟簧外径与内径,mm;s 为碟簧厚度,mm;h_0 为自由高度,mm;M 的表达式见式(10),其中 C 为外径与内径之比。

$$M=\frac{\left(\frac{C-1}{C}\right)^2}{\pi\left(\frac{C+2}{C-1}-\frac{2}{\ln C}\right)}。\tag{10}$$

式(9)对位移 f 求导,得刚度-位移表达式:

$$K=\left(\frac{4Es^3}{(1-\mu^2)MD^2}\right)\left(\frac{3}{2s^2}f^2-\frac{3h_0}{s^2}f+\frac{h_0^2}{s^2}+1\right)。\tag{11}$$

令 $\bar{f}=\frac{f}{s},\bar{h}_0=\frac{h_0}{s},\alpha=\frac{4Es^2}{1-\mu^2},\bar{D}=\frac{D}{s},\bar{K}=\frac{K}{\alpha s}$,则可得无量纲刚度方程:

$$\bar{K}=\frac{1}{M\bar{D}^2}\times(1.5\bar{f}^2-3\bar{h}_0\bar{f}+\bar{h}_0^2+1)。\tag{12}$$

考虑到推力轴承轴向位移的限制,取碟簧的自由高度 $h_0=2.2$ mm。由式(12)可知,无量纲刚度 $\bar{K}$ 可以视为关于无量纲位移 $\bar{f}$ 的二次函数,当高厚比 $\bar{h}_0>\sqrt{2}$ 时出现负刚度区间,因此为保证碟簧具有负刚度特性,取碟簧厚度 $s=1.4$ mm。受限于推力轴承内部尺寸限制,取碟簧外径 $D=60$ mm,同时工程上为了便于与螺旋弹簧并联匹配,碟簧的外径与内径之比 C 一般为 1.7~2.5[14],因此取碟簧内径 $d=26.5$ mm。碟簧的弹性模量 $E=206\ 000$ MPa,泊松比 $\mu=0.3$,则设计的单片碟簧载荷-位移曲线如图 8 所示。

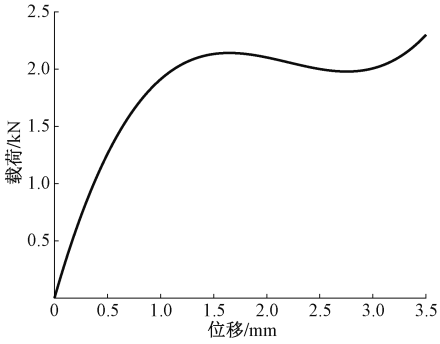

图 8　单片碟簧载荷-位移曲线

Figure 8　Single disc spring load-displacement curve

由图 1 可知,准零刚度隔振器受到载荷时,隔振器的回复力 F_{qzs} 由螺旋弹簧与碟簧的变形共同提供,此时系统的回复力表达式如下:

$$F_{qzs}=K_vf+\frac{4Es^3f}{(1-\mu^2)MD^2}\left[\left(\frac{h_0}{s}-\frac{f}{s}\right)\left(\frac{h_0}{s}-\frac{f}{2s}\right)+1\right]。\tag{13}$$

式中:K_v 为螺旋弹簧的刚度。

令 $\bar{F}_{qzs}=\frac{F_{qzs}}{sK_v},\bar{f}=\frac{f}{s},\bar{h}_0=\frac{h_0}{s},\beta=\frac{4Es}{K_v(1-\mu^2)}$,$\bar{D}=\frac{D}{s}$,则式(13)可写成如下无量纲形式:

$$\bar{F}_{qzs}=\bar{f}+\frac{\beta}{M\bar{D}^2}\left[\frac{1}{2}\bar{f}^3-\frac{3}{2}\bar{h}_0\bar{f}^2+(\bar{h}_0^2+1)\bar{f}\right]。\tag{14}$$

根据分析,设计一个刚度为 200 000 N/m 的螺旋弹簧与碟簧并联,构建单个准零刚度隔振器,并将 4 个准零刚度隔振器嵌入推力轴承,进行推进轴系的纵向隔振。图 9 为准零刚度隔振器载荷-位移的设计曲线与仿真曲线对比,曲线的吻合度好,因此设计的碟簧与螺旋弹簧并联后,准零刚度隔振器的非线性刚度值能达到预设的 1×10^{12} N/m^3。

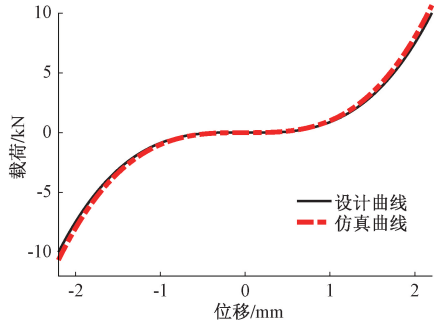

图 9　准零刚度隔振器载荷-位移曲线

Figure 9　Quasi-zero stiffness isolator load-displacement curve

3.3 阻尼比对系统稳定性的影响

确定非线性刚度参数后,进一步分析不同阻尼比 ζ_2 对系统响应稳定性的影响,如图 10 所示。图 10(a)、10(b)、10(c)分别表示了选取不同阻尼比 ζ_2 时,系统的幅频响应与不稳定区间。图 10(d)表示激励力幅值为 75 N 时,系统的幅频响应随阻尼比 ζ_2 变化的曲线。

由图 10 可知,阻尼比 ζ_2 越大,系统幅频响应曲线与不稳定区间的交集越小,当阻尼比 ζ_2 取 0.05 并且激励力幅值小于 75 N 时,系统的幅频响应曲线不再出现不稳定的区间,这表明此时系统不会出现跳跃现象而影响隔振效果。此外在激励力幅值一定时,增大阻尼比能有效抑制共振峰的峰值,并且降低起始隔振频率。因此选取阻尼比 ζ_2 为 0.05。

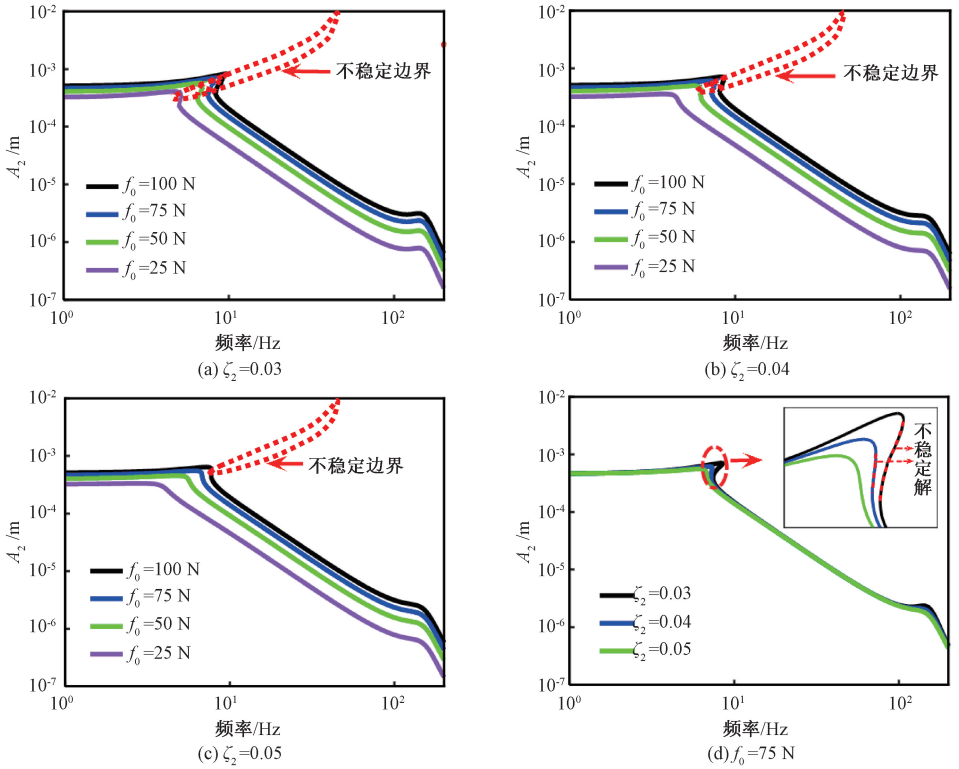

图 10 不同阻尼比幅频响应与稳定性图

Figure 10 Amplitude-frequency response and stability diagram of different damping ratios

4 隔振性能分析

准零刚度隔振器的非线性刚度与阻尼比分别取 1×10^{12} N/m^3、0.05 时系统的力传递率曲线如图 11 实线所示,图 11 中虚线表示无隔振器系统的力传递率。

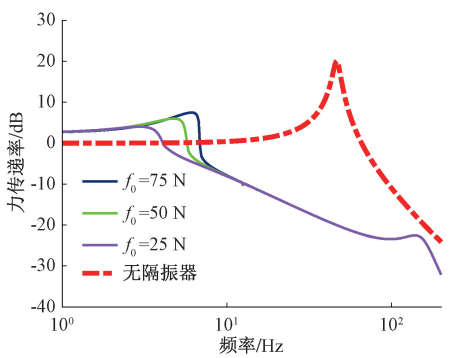

图 11 不同激励力幅值条件下系统力传递率曲线

Figure 11 System force transmission rate curve in different excitation force amplitude conditions

由图 11 可知,对于无隔振器的线性系统而言,其力传递率与激励力幅值无关;而对含准零刚度隔振器的系统而言,减小激励力幅值,其力传递率响应峰值与一阶固有频率均减小。将激励力幅值控制在较小范围内时,准零刚度隔振器能够有效隔离 10~200 Hz 的振动,并且力传递率曲线不再出现跳跃现象。这说明设计的准零刚度隔振器具有高承载、低频隔振性能好的优点。

5 结论

针对船舶推进轴系纵向低频隔振难的问题,将准零刚度隔振器内嵌入船舶的推力轴承。在设计准零刚度隔振器时,综合考虑系统响应的稳定性与轴系纵向静变形的限制,确定了准零刚度隔振器的具体参数。通过静力学分析获得了碟簧与螺旋弹簧相应的结构与力学参数,得出以下结论:当准零刚度隔振器的非线性刚度与阻尼比分别为 1×10^{12} N/m^3、

0.05 时,系统稳态响应的解在 200 Hz 内都是稳定的;在承受 10 000 N 载荷时,可以有效隔离 10~200 Hz 的振动。

参考文献:

[1] 赵耀, 张赣波, 李良伟. 船舶推进轴系纵向振动及其控制技术研究进展[J]. 中国造船, 2011, 52(4): 259-269.
ZHAO Y, ZHANG G B, LI L W. Review of advances on longitudinal vibration of ship propulsion shafting and its control technology[J]. Shipbuilding of China, 2011, 52(4): 259-269.

[2] GOODWIN A J H. The design of a resonance changer to overcome excessive axial vibration of propeller shafting [J]. Transactions of the institute of marine engineers, 1960, 72: 37-63.

[3] DYLEJKO P G, KESSISSOGLOU N J, TSO Y, et al. Optimisation of a resonance changer to minimise the vibration transmission in marine vessels[J]. Journal of sound and vibration, 2007, 300(1/2): 101-116.

[4] MERZ S, KINNS R, KESSISSOGLOU N. Structural and acoustic responses of a submarine hull due to propeller forces[J]. Journal of sound and vibration, 2009, 325(1/2): 266-286.

[5] 储炜, 赵耀, 张赣波, 等. 共振转换器的动力反共振隔振理论与应用[J]. 船舶力学, 2016, 20(增刊 1): 222-230.
CHU W, ZHAO Y, ZHANG G B, et al. Dynamic anti-resonance vibration isolation theory of resonance changer and application[J]. Journal of ship mechanics, 2016, 20(S1): 222-230.

[6] 胡泽超, 何琳, 徐伟, 等. 船舶推进轴系纵向振动共振转换器的优化设计[J]. 中国舰船研究, 2019, 14(1): 107-113.
HU Z C, HE L, XU W, et al. Optimzation design of resonance changer for marine propulsion shafting in longitudinal vibration[J]. Chinese journal of ship research, 2019, 14(1): 107-113.

[7] 刘扭扭. 基于动力反共振的推进轴系纵向振动控制方法研究[D]. 上海: 上海交通大学, 2019.
LIU N N. Investigation on longitudinal vibration control method of the shafting system based on dynamic antiresonance vibration isolator[D]. Shanghai: Shanghai Jiao Tong University, 2019.

[8] 吴明亮, 赵晨名, 张来喜. 准零刚度振动控制系统的研究进展[J]. 南京理工大学学报, 2021, 45(1): 18-26.
WU M L, ZHAO C M, ZHANG L X. Research progress of quasi-zero stiffness vibration control system[J]. Journal of Nanjing university of science and technology, 2021, 45(1): 18-26.

[9] CARRELLA A, BRENNAN M J, KOVACIC I, et al. On the force transmissibility of a vibration isolator with quasi-zero-stiffness[J]. Journal of sound and vibration, 2009, 322(4/5): 707-717.

[10] LE T D, AHN K K. A vibration isolation system in low frequency excitation region using negative stiffness structure for vehicle seat[J]. Journal of sound and vibration, 2011, 330(26): 6311-6335.

[11] HUANG X C, LIU X T, HUA H X. Effects of stiffness and load imperfection on the isolation performance of a high-static-low-dynamic-stiffness non-linear isolator under base displacement excitation[J]. International journal of non-linear mechanics, 2014, 65: 32-43.

[12] SUN X T, JING X J. Analysis and design of a nonlinear stiffness and damping system with a scissor-like structure [J]. Mechanical systems and signal processing, 2016(66/67): 723-742.

[13] WANG X L, ZHOU J X, XU D L, et al. Force transmissibility of a two-stage vibration isolation system with quasi-zero stiffness[J]. Nonlinear dynamics, 2017, 87(1): 633-646.

[14] 白晓辉, 白鸿柏, 郝慧荣. 碟形弹簧负刚度在低频精密隔振中的应用研究[J]. 新技术新工艺, 2009(10): 24-27.
BAI X H, BAI H B, HAO H R. Application research on the negative stiffness of disk spring used in low frequency precision vibration isolation[J]. New technology & new process, 2009(10): 24-27.

[15] MENG L S, SUN J G, WU W J. Theoretical design and characteristics analysis of a quasi-zero stiffness isolator using a disk spring as negative stiffness element[J]. Shock and vibration, 2015, 2015: 813763.

[16] 孟令帅, 孙景工, 牛福, 等. 新型准零刚度隔振系统的设计与研究[J]. 振动与冲击, 2014, 33(11): 195-199.
MENG L S, SUN J G, NIU F, et al. Design and analysis of a novel quasi-zero stiffness vibration isolation system [J]. Journal of vibration and shock, 2014, 33(11): 195-199.

[17] 张阳阳, 所俊. 推力轴承隔振对潜艇声振特性影响研究[J]. 噪声与振动控制, 2020, 40(3): 240-245.
ZHANG Y Y, SUO J. Study on the influence of thrust bearing isolation on the acoustic and vibration characteristics of submarines[J]. Noise and vibration control, 2020, 40(3): 240-245.

[18] ALMEN J O. The uniform-section disk spring[J]. Transactions of the American society of mechanical engineers, 1936,58:305-314.

(下转第 64 页)

Spectrum Analysis and Seismic Evaluation of Support and Hanger of Suspension Air Conditioning Unit

WANG Hehui[1], LIU Yuxin[1], TANG Yi[2], ZHU Jinlin[2], PAN Jian[2]

(1. School of Mechanical and Power Engineering, East China University of Science and Technology, Shanghai 200237, China; 2. Shanghai Installation Engineering Group Co., Ltd., Shanghai 200080, China)

Abstract: Based on the response spectrum analysis method, ANSYS finite element software and its APDL programming, the three-dimensional finite element model that could fully reflect the structural characteristics was established by using the spatial beam element, 3D longitudinal spring damping element and solid element. And the seismic calculation of support and hanger of an air conditioning unit in suspension installation mode was carried out. Considering the static load and OBE seismic load, the static analysis was carried out firstly, and then the modal analysis and multi-point response spectrum analysis of OBE seismic load were carried out. Finally, according to the calculation results of static analysis and spectrum analysis by the square root of sum square method (SRSS method) of the modal combination, based on ASME AG-1 codes, the strength and stiffness of support and hanger were subjected to seismic evaluation. The results showed that with the combination of static load and OBE seismic load, the tensile stress, shear stress, bending stress and tensile-bending combination of the support and hanger were less than the stress limit, and had a wide margin of safety. Most of the displacement of the support and hanger come from the rigid displacement of the whole system caused by the shrinkage of spring dampers, and the rest came from the relative displacement of the channel steel bottom frame, both of which could meet the requirements and have a large safety margin. Expansion bolts at the root of the support and hanger were mainly affected by the tension, and their strength could meet the requirements and the safety margin was large. The evaluation showed that the support and hanger of the suspended air conditioning unit had sufficient seismic strength and stiffness.

Keywords: suspension air conditioning unit; support and hanger; spectrum analysis; ASME AG-1 codes; safety assessment

---

(上接第57页)

Research on Longitudinal High Load-bearing Quasi-zero Stiffness Isolator for Propulsion Shafting

REN Zhiying[1,2], QIU Tao[1,2], LIU Niuniu[1,2], BAI Hongbai[1,2], YAO Jiecheng[1,2], LIANG Yi[1,2]

(1. School of Mechanical Engineering and Automation, Fuzhou University, Fuzhou 350116, China; 2. Institute of Metal Rubber, Vibration and Noise, Fuzhou University, Fuzhou 350116, China)

Abstract: Aiming at the problem of longitudinal low-frequency vibration isolation of ship propulsion shafting, a high-load quasi-zero stiffness isolator was designed based on disc spring with negative stiffness characteristics and positive-stiffness coil spring in parallel. The dynamic equation of the shafting-quasi-zero stiffness vibration isolation system was established. Through the harmonic balance method, the steady-state response of the system was solved, and the validity of the solution was verified by numerical calculation. For the problem of system response stability, firstly, the influence of nonlinear stiffness of quasi-zero stiffness isolator and external excitation force amplitude on response stability were studied, and combined with the longitudinal static deformation of the shafting, the nonlinear stiffness was determined. Then the specific structural and mechanical parameters of the disc spring and the coil spring were obtained through static analysis. Finally, the influence of damping ratio of quasi-zero stiffness isolator and external excitation force amplitude on the response stability of the system were analyzed, the damping ratio was determined. The results showed that when the nonlinear stiffness and damping ratio were taken as 1×10^{12} N/m^3 and 0.05, respectively, the main resonance of the system no longer jumps, and the solution of the steady-state response of the system was stable within 200 Hz. In the meantime, even with a load of 10 000 N, the quasi-zero stiffness isolator could still effectively isolate the vibration in the range of 10 Hz to 200 Hz.

Keywords: propulsion shafting; low frequency vibration isolation; disc spring; quasi-zero stiffness; stability